Frontiers of Information Technology & Electronic Engineering
www.zju.edu.cn/jzus; engineering.cae.cn; www.springerlink.com
ISSN 2095-9184 (print); ISSN 2095-9230 (online)
E-mail: jzus@zju.edu.cn

Series transformer based diode-bridge-type solid state fault current limiter

Amir HEIDARY[1], Hamid RADMANESH[†‡2,3], Seyed Hamid FATHI[2], G. B. GHAREHPETIAN[2]

([1]*Electrical Engineering Department, Islamic Azad University, Takestan Branch, Takestan, Iran*)

([2]*Electrical Engineering Department, Amirkabir University of Technology, Tehran, Iran*)

([3]*Electrical Engineering Department, Aeronautical University of Science and Technology, Tehran, Iran*)

[†]E-mail: hamid.radmanesh@aut.ac.ir

Received Dec. 15, 2014; Revision accepted Apr. 16, 2015; Crosschecked Aug. 7, 2015

Abstract: We propose a novel series transformer based diode-bridge-type solid state fault current limiter (SSFCL). To control the fault current, a series RLC branch is connected to the secondary side of an isolation series transformer. Based on this RLC branch, two current limiting modes are created. In the first mode, R and C are bypassed via a paralleled power electronic switch (insulated-gate bipolar transistor, IGBT) and L remains connected to the secondary side of the transformer as a DC reactor. In the second mode, the series reactor impedance is not enough to limit the fault current. In this case, the fault current can be controlled by selecting a proper on-off duration of the parallel IGBT, across the series damping resistor (*R*) and capacitor, which inserts high impedance into the line to limit the fault current. Then, by controlling the magnitude of the DC reactor current, the fault current is reduced and the voltage of the point of common coupling (PCC) is kept at an acceptable level. In addition, in the new SSFCL, the series RC branch, connected in parallel with the IGBT, serves as a snubber circuit for decreasing the transient recovery voltage (TRV) of the IGBT during on-off states. Therefore, the power quality indices can be improved. The measurement results of a built prototype are presented to support the simulation and theoretical studies. The proposed SSFCL can limit the fault current without any delay and successfully smooth the fault current waveform.

Key words: Solid state fault current limiter (SSFCL), Power quality, Voltage sag, Point of common coupling (PCC), Isolation transformer

doi:10.1631/FITEE.1400428 **Document code:** A **CLC number:** TM471

1 Introduction

Nowadays, economic growth causes an exponential increase in electrical power generation. To supply the demand, new power generation plants are installed and their interconnections may increase the short-circuit ratings and result in fault currents that are more than the maximum short-circuit capacity of the switchgears. Among the various faults occurring in distribution systems, the short-circuit fault is the most probable one and can cause serious damage to the network equipment. The short-circuit fault can cause overvoltage transients, loss of synchronization, insulation failure, and may even cause an explosion of equipment containing insulating oil. There are some solutions, such as upgrading and replacing switchgears (McAullife *et al.*, 2001), connecting a power electronic (PE) convertor as an interface between networks and the installed distributed generator (DG) (Hanif and Choudhry, 2009) and fuses (Wu *et al.*, 2001). As a reliable, self-triggering, cheap equipment, the fuse can interrupt fault currents without using sensors or actuators (Cheng *et al.*, 2014). The major disadvantage is its single use nature, and thus it needs to be manually replaced. Connecting the PE converter interface between the network and

‡ Corresponding author
ORCID: Amir HEIDARY, http://orcid.org/0000-0001-8234-6387; Hamid RADMANESH, http://orcid.org/0000-0002-3261-642X

newly installed DG causes a higher power rating, weight, and cost, if it is used as a fault current limiter (FCL) (Ghanbari and Farjah, 2013). The next most popular solution is a power system reconfiguration, but this method may decrease network power quality due to higher total system losses and source impedances (Amanulla *et al.*, 2012). A circuit breaker (CB) is a protective equipment that can be 'tripped' and reset either automatically or manually. However, CBs with high-current interrupting capabilities are expensive. The CBs require high maintenance and have a limited lifetime (Vintan, 2008). In recent years, novel schemes for limiting the magnitude of the fault current have been proposed. The FCL is the best solution for fault current limitation. FCLs are classified by their principles of operation. They can be implemented with passive or active and linear or nonlinear elements (Iwahara *et al.*, 1999), inductive devices (Yamaguchi and Kataoka, 2008), vacuum switches (Zhao *et al.*, 2010), semiconductor power electronic switches (Jafari *et al.*, 2011), and superconductor technologies (Du *et al.*, 2011; Fani *et al.*, 2011; Na *et al.*, 2012). Hybrid structures have also been reported (Jang *et al.*, 2010). The FCLs limit the amplitude of the short-circuit current, improve power system transient stability, power quality, reliability, and decrease inrush current in transformers (Tsuda *et al.*, 2001; Ye *et al.*, 2002; Hagh and Abapour, 2007; 2009b; Liu *et al.*, 2007; Cvoric *et al.*, 2008; Abramovitz and Smedley, 2012; Firouzi *et al.*, 2013; Madani *et al.*, 2013). An ideal FCL should have zero impedance in its normal operation mode, high impedance during fault conditions, quick response to fault occurrence, fast recovery after fault clearance, acceptable reliability, and also low cost (Hagh and Abapour, 2009a). Bridge-type FCLs use a current fed full-bridge converter. This topology is inherently suitable for using switches (diodes, thyristors, or other power electronic switches) as line commutated switches (Radmanesh *et al.*, 2015a).

In this paper, the proposed solid state FCL (SSFCL) has a simple and applicable structure, which can limit the magnitude of the fault current to a certain and safe value. Also, the proposed structure can reduce the harmonic distortion and switching overvoltages, and adjust the PCC voltage. The comparative study of the suggested SSFCL with the FCL presented in Hagh and Abapour (2009b) shows its superior characteristics. The SSFCL operation in normal and faulty conditions is studied and the experimental prototype clearly confirms the simulation results.

2 Electrical network topology

A single-line diagram of an electrical network including the proposed SSFCL is as shown in Fig. 1. The proposed network includes two feeders, and it is assumed that feeder F1 supplies a sensitive load and feeder F2 delivers power to other loads.

An isolating transformer is the main part of the SSFCL. Its primary winding is connected in series with the line, and the secondary winding is connected to a single-phase diode-bridge rectifier 1. The transformer is used as a series transformer and its winding ratio is equal to one. The rectifier bridge (D_1–D_4) provides a DC power source for short-circuiting the DC reactor (L_d) during the normal operation mode. The RLC branch is used as an SSFCL component where C and a small part of resistance R form a snubber circuit for IGBT. L_d is a non-superconductor

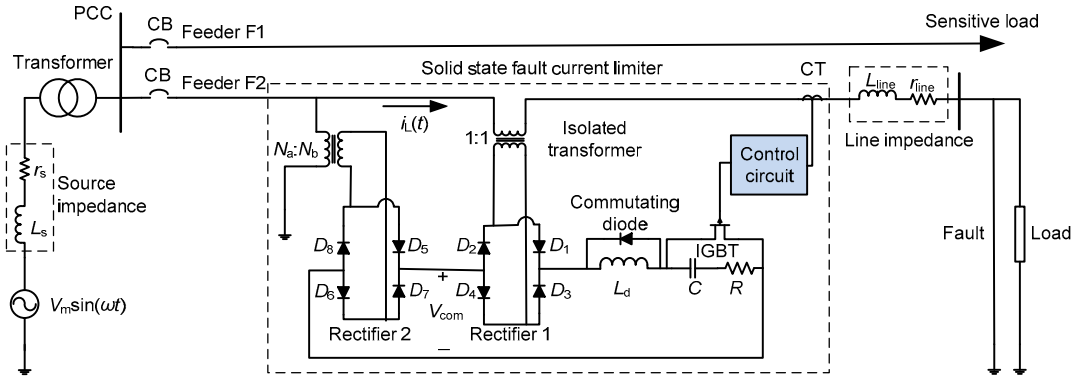

Fig. 1 Single-line diagram of the electrical network including the proposed SSFCL

coil and is used as a DC reactor. Its resistance and inductance are modeled by r_d and L_d, respectively.

The IGBT is the main component of the proposed SSFCL. By its proper switching, the overcurrent amplitude is controlled. The DC-bias voltage source includes a voltage transformer and a rectifier bridge (D_5–D_8). The voltage transformer is a step-down transformer with an N_a/N_b turns ratio and feeds the D_5–D_8 for providing a proper DC voltage. This DC voltage is used for compensation of power losses during the normal operation mode. The power losses during the normal operation mode include rectifier bridge 1 power loss, IGBT on-state power loss, and isolated transformer loss. Connecting the DC-bias voltage source in series with the DC reactor can compensate for power losses during the normal operation mode, because it charges the DC reactor slightly higher than the peak current of the line voltage and causes a short circuit in the DC reactor.

3 SSFCL operation principles

The principles of the SSFCL operation can be divided into three modes: normal operation, fault, and freewheeling.

3.1 Normal operation mode

After closing the CB, diode pairs D_1–D_4 and D_2–D_3 conduct for positive and negative cycles, respectively and form a charging period. During the charging period, the line current is larger than the DC reactor current and the on-state diodes charge the DC reactor. During the discharging mode, the DC reactor current is larger than the line current and its current freewheels via a rectifier bridge and all diodes (D_1–D_4) conduct. After some charging and discharging modes, the DC voltage of the bridge output charges the DC reactor with a DC current and short-circuits the DC reactor. In this case, the IGBT is on, so both the damping resistor and capacitor are bypassed and the secondary side of the series transformer is short-circuited. In this way, the proposed SSFCL has negligible effect on the network voltage and load current, and the DC-bias voltage source compensates for the SSFCL power losses and improves the load voltage and line current power quality.

3.2 Fault mode

When a downstream short-circuit fault occurs, the rising fault current flows through the DC reactor after being rectified by the rectifier bridge. Therefore, the reactor reacts against the current rise and limits the increase rate of the fault current, depending on the value of L_d. If the fault remains for a long time, the current through the DC reactor will increase beyond the threshold current level (i_T). In this case, the controller circuit controls the on and off durations of the IGBT, and inserts the series RC branch into the current path to keep the DC reactor current below a specified level. Through turning off the IGBT, the series capacitor and damping resistor absorb the stored energy in the SSFCL inductance, resulting in a decreased DC reactor current. When the IGBT is turned on, the DC reactor current increases. So, using suitable on and off durations of the IGBT, it is possible to keep the DC reactor current below the threshold level for a given damping resistor value. By controlling the DC reactor current, it is possible to reduce the inductance and current rating of the DC reactor. Decreasing the DC reactor size and connecting the DC-bias voltage source can improve the PCC voltage quality and load current due to compensation of SSFCL power losses. Also, the damping resistor and capacitor serve as an RC snubber circuit and reduce the IGBT transient recovery voltage (TRV) during the fault period.

3.3 Freewheeling mode

After suppressing the fault current, the IGBT bypasses the RC branch again and the DC reactor discharges rapidly via the rectifier diodes, DC reactor resistance, and commutating diode. In this mode, the SSFCL operates in a discharging mode and the DC reactor acts as a short circuit. After discharging the DC reactor, the SSFCL shows negligible impedance in the line and the electrical load seems to be directly connected to the line.

4 Analytical study

The SSFCL analytical study is divided into two modes, namely normal and fault modes.

4.1 Normal operation mode

During the normal mode, the DC reactor behavior includes both charging and discharging periods. During the charging mode, D_1 and D_2 are in on-state and the line current is the same as the DC reactor current as shown in Fig. 2a. We have

$$V\sin(\omega t)=ri_{\mathrm{L}}(t)+L\frac{\mathrm{d}i_{\mathrm{L}}(t)}{\mathrm{d}t}+2V_{\mathrm{DF}}. \tag{1}$$

Solving Eq. (1) gives the following answer for the line current in the charging mode:

$$i_{\mathrm{L}}(t)=\exp\left[-\frac{r}{L}(t-t_0)\right]\left[i_0-\frac{V}{Z}\sin(\omega t_0-\varphi)+\frac{2V_{\mathrm{DF}}-V_{\mathrm{com}}}{r}\right]+\frac{V}{Z}\sin(\omega t-\varphi)-\frac{2V_{\mathrm{DF}}-V_{\mathrm{com}}}{r}, \tag{2}$$

where V is the source voltage, L includes source (L_{s}), line (L_{L}), DC reactor (L_{d}), and load (L_{Load}) inductances, and r models the source (r_{s}), line (r_{L}), load (r_{Load}), and reactor (r_{d}) resistances. In addition, $i_{\mathrm{L}}(t)=i_{\mathrm{d}}(t)=i(t)$, $Z=\sqrt{r^2+(\omega L)^2}$, $\varphi=\arctan(\omega L/r)$, $i_0=i(t_0)$, V_{com} is the DC-bias voltage source amplitude, and V_{DF} is the voltage drop on the rectifier diode.

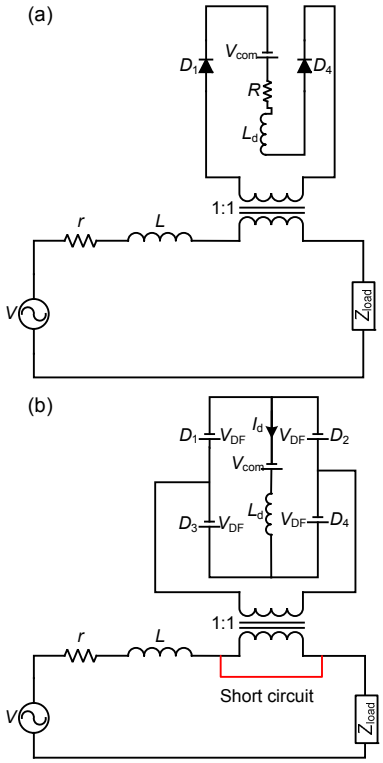

Fig. 2 Electrical network equivalent circuit in the normal mode: (a) charging mode; (b) discharging mode

During the discharging mode, the DC reactor current is more than the line current, all diodes (D_1–D_4) are in on-state, and the DC reactor current freewheels via them (Fig. 2b). In this case, IGBT is on, RC branch is bypassed, induced DC voltage on the DC reactor is bypassed as well, and the DC-bias voltage source compensates for the SSFCL power losses. Furthermore, the secondary side of the series isolated transformer is bypassed, which results in negligible impedance seen from the primary side of the transformer. By neglecting the series transformer leakage impedance, the equivalent circuit of the distribution network of Fig. 1 from the viewpoint of feeder F2, is an inductance (L) and a resistance (r) in series with the electrical voltage source (Fig. 2b).

The line current during the discharging mode is obtained by solving Eq. (3):

$$V\sin(\omega t)=L\frac{\mathrm{d}i_{\mathrm{L}}(t)}{\mathrm{d}t}+ri_{\mathrm{L}}(t). \tag{3}$$

The source voltage of the electrical network is sinusoidal with angular frequency ω and amplitude V_{m}. The solution of Eq. (3) is given in Eq. (4):

$$i_{\mathrm{L}}(t)=\exp\left[-\frac{r}{L}(t-t_2)\right]\left[i_2-\frac{V}{Z}\sin(\omega t_2-\varphi)\right]+\frac{V}{Z}\sin(\omega t-\varphi), \tag{4}$$

where $Z=\sqrt{r^2+(\omega L)^2}$, $\varphi=\arctan(\omega L/r)$, $i_2=i(t_2)$, V is the source voltage, L includes source (L_{s}), line (L_{L}), and load (L_{Load}) inductances, and r models source (r_{s}), line (r_{L}), and load (r_{Load}) resistances. In the discharging mode, the DC reactor current and line current have different values. The DC reactor current during the discharging mode can be obtained by solving

$$L_{\mathrm{d}}\frac{\mathrm{d}i_{\mathrm{d}}(t)}{\mathrm{d}t}+r_{\mathrm{d}}i_{\mathrm{d}}(t)+2V_{\mathrm{DF}}-V_{\mathrm{com}}=0, \tag{5}$$

$$i_{\mathrm{d}}(t)=\exp\left(-\frac{r_{\mathrm{d}}}{L_{\mathrm{d}}}(t-t_2)\right)\left(i_2+\frac{2V_{\mathrm{DF}}-V_{\mathrm{com}}}{r_{\mathrm{d}}}\right)-\frac{2V_{\mathrm{DF}}-V_{\mathrm{com}}}{r_{\mathrm{d}}}. \tag{6}$$

4.2 Faulty operation mode

During the faulty operation mode, when the current magnitude increases beyond the specified level (I_L), IGBT is turned off and the series RC branch is placed into the secondary side of the series transformer, causing the current to decrease below the threshold value (I_T). In this case, IGBT is turned on again and bypasses the series RC branch. By suitable control of the IGBT's on and off durations, the fault current is kept below the threshold level. When the IGBT is off, the RLC branch is connected to the secondary side of the transformer and SSFCL operates in the charging mode. To analyze the system behavior during the fault mode and in the case of the charging period the equivalent circuit of the system (Fig. 3a) is used.

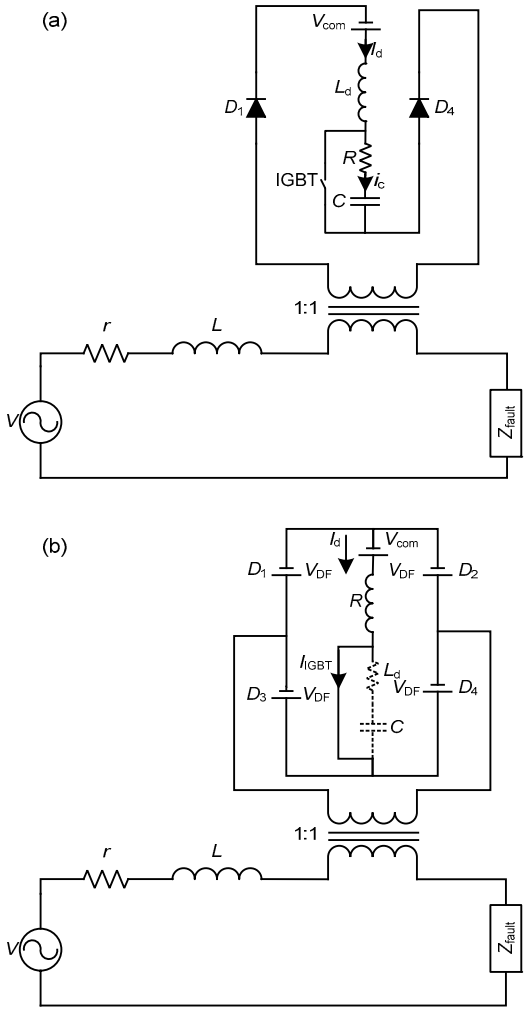

Fig. 3 Electrical network equivalent circuit during fault: (a) charging mode; (b) discharging mode

Considering Fig. 3a and isolating the transformer with a unity turns ratio, the equivalent circuit of the distribution network is a series RLC circuit. The differential equation of the circuit shown in Fig. 3a is given as follows:

$$ri_C(t)+L\frac{\mathrm{d}i_C(t)}{\mathrm{d}t}+V_C(t)=V_m\sin(\omega t+\varphi)+V_{com}-2V_{DF}, \quad (7)$$

where V_{com} is equal to the DC-bias voltage source, V_{DF} is the voltage drop across the diode, $V_C(t)$ is the voltage on the series capacitor, $L=L_s+L_{line}+L_d+L_f$, and L_s, L_{line}, L_d, and L_f are the inductances of the source, line, DC reactor, and fault, respectively, $r=r_s+r_{line}+r_d+R+r_f$, and r_s, r_{line}, r_d, R, and r_f are the resistances of the source, line, DC reactor, damping resistor, and fault, respectively. Assume that the circuit breaker is energized at t_0, IGBT is opened at t_5, and the initial conditions are given as follows:

$$i_C(t_5)=I_5,\ V_C(t_5)=V_5, \quad (8)$$

$$\frac{\mathrm{d}i_C(t_5)}{\mathrm{d}t}=\frac{V_m\sin(\omega t_5+\varphi)-V_5-rI_5}{L}. \quad (9)$$

The capacitor current can be obtained by solving Eq. (7):

$$i_C(t)=\frac{V_m}{Z}\sin(\omega t+\varphi-\varphi_1)+i_{n1}(t), \quad (10)$$

where $Z=\sqrt{r^2+[\omega L-(\omega C)^{-1}]^2}$, $\varphi_1=\arctan\{[\omega L-(\omega C)^{-1}]/r\}$, and $i_{n1}(t)$ is the natural response of the circuit shown in Fig. 3a. As mentioned before, the turns ratio of the series transformer is equal to 1, and there are three types of natural responses, which are associated with the system parameters. The solutions for the natural responses in the limiting mode are given as follows:

1. The over-damped response is

$$i_{n1}(t)=A\exp[S_1(t-t_5)]+B\exp[S_2(t-t_5)], \quad (11)$$

where $S_1=-\alpha+\sqrt{\alpha^2-\omega_0^2}$, $S_2=-\alpha-\sqrt{\alpha^2-\omega_0^2}$, $\alpha=r/(2L)$, and $\omega_0=1/\sqrt{LC}$. The coefficients A and B can be obtained as follows:

$$A=\frac{V_{\mathrm{m}}}{2Z\sqrt{\alpha^2-\omega_0^2}}\left[S_2\sin(\omega t_5+\varphi-\varphi_1)\right.$$
$$\left.-\omega\cos(\omega t_5+\varphi-\varphi_1)\right] \quad (12)$$
$$+\frac{\alpha V_{\mathrm{m}}\sin(\omega t_5+\varphi)-\alpha V_5+V_{\mathrm{com}}-2V_{\mathrm{DF}}}{2\alpha L\sqrt{\alpha^2-\omega_0^2}},$$

$$B=\frac{-V_{\mathrm{m}}}{2Z\sqrt{\alpha^2-\omega_0^2}}\left[S_1\sin(\omega t_5+\varphi-\varphi_1)\right.$$
$$\left.-\omega\cos(\omega t_5+\varphi-\varphi_1)\right] \quad (13)$$
$$-\frac{\alpha V_{\mathrm{m}}\sin(\omega t_5+\varphi)-\alpha V_1+V_{\mathrm{com}}-2V_{\mathrm{DF}}}{2\alpha L\sqrt{\alpha^2-\omega_0^2}}.$$

2. The critically damped response is

$$i_{\mathrm{n1}}(t)=A\exp[\alpha(t-t_5)]+B(t-t_0)\exp[-\alpha(t-t_5)]. \quad (14)$$

The coefficients A and B can be obtained as follows:

$$A=\frac{-V_{\mathrm{m}}}{Z}\sin(\omega t_5+\varphi-\varphi_1), \quad (15)$$

$$B=\frac{-V_{\mathrm{m}}}{Z}\left[\alpha\sin(\omega t_5+\varphi-\varphi_1)+\omega\cos(\omega t_5+\varphi-\varphi_1)\right]$$
$$-\frac{\alpha V_{\mathrm{m}}\sin(\omega t_5+\varphi)-\alpha V_5+V_{\mathrm{com}}-2V_{\mathrm{DF}}}{\alpha L}. \quad (16)$$

3. The under-damped response is

$$i_{\mathrm{n1}}(t)=\mathrm{e}^{-\alpha(t-t_5)}\left\{A\sin[\omega_{\mathrm{d}}(t-t_5)]+B\cos[\omega_{\mathrm{d}}(t-t_5)]\right\}, \quad (17)$$

where $\omega_{\mathrm{d}}=\sqrt{\omega_0^2-\alpha^2}$, and the coefficients A and B can be obtained as

$$A=\frac{-V_{\mathrm{m}}}{Z\omega_{\mathrm{d}}}\left[\alpha\sin(\omega t_5+\varphi-\varphi_1)+\omega\cos(\omega t_5+\varphi-\varphi_1)\right]$$
$$+\frac{\alpha V_{\mathrm{m}}\sin(\omega t_5+\varphi)-\alpha V_1+V_{\mathrm{com}}-2V_{\mathrm{DF}}}{\alpha\omega_{\mathrm{d}}L}, \quad (18)$$

$$B=\frac{-V_{\mathrm{m}}}{Z}\sin(\omega t_5+\varphi-\varphi_1). \quad (19)$$

Considering the system parameters, the solution for the natural response is an under-damped response. The capacitor voltage in the faulty operation mode shows three exponential components. The transient responses are damped after several milliseconds considering the system time constant.

4.3 Freewheeling mode

As mentioned before, during this mode, the DC reactor current is more than the line current, and according to Fig. 3b, D_1 and D_3 of the rectifier bridge carry $(i_{\mathrm{d}}+i_{\mathrm{line}})/2$, and D_3 and D_4 carry $(i_{\mathrm{d}}-i_{\mathrm{line}})/2$. So, all diodes conduct and the DC reactor discharges. As long as the line current is equal to or lower than that of the DC reactor, D_1 through D_4 are in on-state and the DC reactor current freewheels in the rectifier diodes.

5 Control strategy

The control block diagram of the proposed SSFCL is as shown in Fig. 4.

In the normal mode, the diodes of the bridge legs are on and the line current passes through the short-circuited DC reactor. In this case, the line current (i_{line}) is monitored by the current transformer (CT). It passes the 50 Hz band pass filter and its absolute value is compared with the specified level (I_{L}). During the normal operation mode, there is a small difference between these two currents (i_{line} and I_{L}), and the step generator sends the proper command signal to turn on the IGBT. So, the reactor is charged to the peak value of the line current (i_{line}) and behaves as a short circuit. In the fault inception, i_{line} becomes greater than I_{L} and the control circuit turns off the IGBT. So, the series RC branch is connected

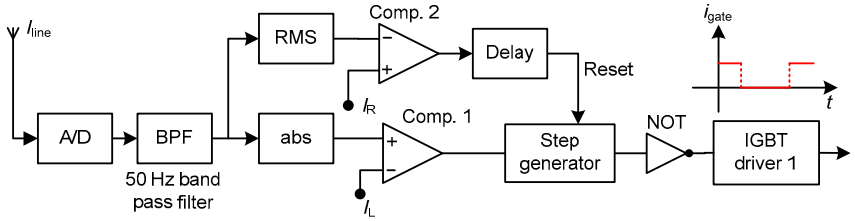

Fig. 4 Control logic block diagram of SSFCL

to the secondary side of the isolation transformer and limits the fault current between I_L and I_T. After fault removal, the line current will instantaneously decrease. To detect the line current reduction, the root mean square (RMS) value of the line current is compared with the RMS reference current (I_R). The value of I_R is set slightly lower than I_L, which allows the controller to detect the fault removal instant. A second control loop can be formed by obtaining a feedback from the line current RMS value. The line current is applied to an RMS calculating block, the output of which is compared with the reference current level (i_R). At the fault removal, while the IGBT is still off, the RMS value of the line current decreases rapidly below the reference value i_R. The detector circuit will then send the reset signal to the step generator block, and this block generates the command signal for the IGBT after a half cycle delay. During this delay, both the damping resistor and electrical load are connected to the network and the DC reactor is discharged rapidly. As a result, the system returns to its normal operation mode.

6 Design consideration

6.1 DC reactor design

The differential equation of the equivalent circuit shown in Fig. 2a without considering the series capacitor or damping resistor is given as follows:

$$V_{DS} = r_d i_d(t) + L_d \frac{\mathrm{d}i_d(t)}{\mathrm{d}t}, \tag{20}$$

where V_{DS} is the voltage drop on the series DC reactor. By solving Eq. (20), the DC reactor current is obtained as

$$i_d(t) = \frac{V_{DS}}{L_d}(t - t_0) + I_{peak}, \tag{21}$$

where the initial value of $i_d(t)$ at t_0 is I_{peak} and the effect of DC reactor losses (r_d) is not considered in Eq. (21), because in comparison with L_d its value is very small. In addition, we have

$$i_0 = i_d(t = t_0) = I_d, \tag{22}$$

where t_0 is the instant of the fault inception and it is assumed that the circuit breaker can open the faulty line at t_1. The DC reactor inductance value during the normal operation mode should be considered large enough, where the DC reactor current flow through the reactor is slightly higher than the normal flow of the AC current through the transmission line. On the other hand, with respect to the nominal values of the power network equipment, the value of the DC reactor inductance should be chosen properly to decrease the fault current to an acceptable level and enables the circuit breaker to successfully open the faulty line. However, increasing the DC reactor inductance increases the time of its discharge after fault clearance and also the system operation delay. By considering t_1 the necessary time for the circuit breaker to open the faulty line after fault inception and i_1 its corresponding current, we can solve Eq. (20) to obtain Eq. (23) for the fault occurrence mode:

$$t_1 - t_0 = \frac{L_d}{r_d} \ln\left(\frac{r_d i_1 - V_{DS}}{r_d i_0 - V_{DS}}\right), \tag{23}$$

where i_1 is determined via circuit breaker alignment and its capability to open the faulty line. On the other hand, the value of i_1 is determined according to the nominal values of the distribution network equipment. In addition, the time difference between t_1 and t_0 shows the circuit breaker time performance before the current of the power electronic diodes exceeds i_1. Furthermore, by determining the rectifier bridge output voltage (V_{DS}), t_0, and t_1, it is possible to design the DC reactor inductance and resistance.

6.2 Power electronic switches

High rating power electronic switches with current ratings up to 24 kA and voltage ratings up to 4 kV are commercially available (Globalspec, 2015). In addition, the available power electronic switches have rather high blocking voltage and current ratings and are relatively easy to parallel and string. At the medium-voltage level, the use of snubber circuits is mandatory, while it is not necessary for a low voltage level. The suggested SSFCL can employ self-turn-off switches for switching implementation in a short time. This makes the suggested SSFCL cost-effective and reliable for distribution network applications. For SSFCL applications in high power

networks, a proper balancing between switch modules and press-packs must be maintained. However, the power electronic diodes and passive components are accessible in different ratings.

6.3 RC snubber circuit

The series RC branch in parallel with the IGBT is effective in turn-off surge voltage of the switching process. It is also effective for oscillation by dv/dt noise. The resistance of the snubber is combined with the damping resistor. Loss in the snubber itself is quite small, so it is suitable for 50 Hz frequency applications. In a high voltage IGBT circuit, it is better to use a small 'RC snubber circuit'. It helps control the parasitic oscillation of the main circuit. In this application, an RC snubber circuit with a 10 nF capacitance and a 50 Ω damping resistor is used for both snubbing and fault current mitigation purposes. The application of the snubber circuit decreases the IGBT overvoltage during the switching process.

6.4 Series isolated transformer

In the SSFCL structure, the isolation transformer is connected in series with the feeder to transfer electrical power to the rectifier bridge, DC reactor, IGBT, and RC branch while isolating these devices from the feeder, usually for electric shock protection. It can also block the transmission of the DC component. Its purpose is to reflect the impedance of the damping resistor and DC reactor into the primary side at the duration of the fault. The turns ratio of the isolated transformer adjusts the insulation levels and current ratings for the rectifier bridge, damping resistor, IGBT switch, and DC reactor. For the FCL equipment connected to the secondary side of the isolated transformer, the higher voltage results in the smaller current capacity. In this study, the turns ratio of the transformer is given as a=1. Without using the series transformer, some problems may occur for the network:

1. The current of the power electronic switches is the same as the line current, and it can cause serious damage in fault cases because these switches are exposed to the transmission line current transients.

2. The power electronic switches experience the network voltage, and voltage transient is a dangerous condition for these switches.

3. The fault current limiter equipment experiences the network transient conditions.

Using the isolation transformer in the SSFCL structure decreases the voltage and current fluctuations on the secondary side of the transformer. In fact, the filtering behavior of the transformer protects the power electronic equipment against the transient conditions. In addition, the transformer turns ratio is a key factor for designing the voltage and current level of the power electronic equipment on the secondary side of the transformer. The series transformer in isolation applications has a small winding turn at the primary side and its core reluctance is little as well (the core length and cross section are small). The inductance of the primary side is little and its magnetic inductance is considerably small. In addition, the core resistance is considerable, which decreases the core losses and inductive current of the core. However, at fault inception, the isolation transformer should withstand the fault current during the transient state. Because this period is around one fourth of a cycle, the silicon iron core of the transformer cannot be driven into saturation during this period, and its winding must withstand the electromagnetic force as well. The short-circuit (S.C) and open-circuit (O.C) tests of the transformer can determine the equivalent short-circuit impedance and the core loss, respectively. Note that from the O.C test data we can obtain the parallel branch impedances, namely the magnetizing reactance and the resistance representing the core loss referring to the side where measurements have been taken. Due to the transformer parameters, the magnetizing current, core loss, and leakage impedances can be obtained. The isolated transformer is short-circuited during the normal operation mode, and it can insert the SSFCL components in series with the line during the fault period. The magnitude of the short-circuit impedance referring to the primary side of the isolated transformer is $|Z_{\mathrm{eq,CT}}|$. During the normal operation, the voltage drop across the primary side is given as

$$V_{\mathrm{primary}} = \left|Z_{\mathrm{eq,CT}}\right| i_{\mathrm{line,rms}}, \tag{24}$$

where $i_{\mathrm{line,rms}}$ is the RMS value of the line current during the normal operation mode. Therefore, the apparent power of the isolated transformer during the normal operation mode is

$$S_{\mathrm{CT}} = \left|Z_{\mathrm{eq,CT}}\right| i_{\mathrm{line,rms}}^2. \tag{25}$$

However, the main problem of the isolation transformer is its loss during the normal operation mode. By proper design, the isolation transformer core loss can be effectively reduced and in this study, we can consider the isolated transformer an ideal transformer and the transient inrush current on it is negligible. Normally the series isolated transformer would not have a leakage impedance of more than 3%–4% (Radmanesh *et al.*, 2015b). Therefore, the isolated transformer can be considered an ideal transformer and its short-circuit impedance can be neglected as well.

7 Power dissipation

To reduce the power losses during the normal operation mode, the DC-bias voltage source operates at the instant of circuit breaker energization. In this case, the proposed SSFCL has power losses on the DC reactor, DC-bias voltage source, IGBT switch, isolating transformer, and rectifier bridge, as described in the following.

7.1 Rectifier bridge

During the normal operation mode, the DC reactor is short-circuited and all diodes are in on-state. So, the rectifier bridge power loss is

$$P_{\text{loss,RB}} = 4V_{\text{DF}}I_{\text{average}}, \tag{26}$$

where I_{average} is the average current of the diodes in each cycle, equal to I_{peak}/π.

7.2 Series isolated transformer

The short- and open-circuit tests of the isolated transformer can determine the equivalent short-circuit impedance and its core loss, respectively. So, the power loss resulting from the isolated transformer during the normal operation mode can be expressed as follows:

$$P_{\text{loss,CT}} = P_{\text{core,CT}} + R_{\text{eq,CT}}i_{\text{line,rms}}^2, \tag{27}$$

where $P_{\text{core,CT}}$ is the core loss and $R_{\text{eq,CT}}$ is the equivalent resistance referring to the primary side.

7.3 DC reactor

The DC reactor loss is modeled by r_{d}, and its power loss during the normal operation mode can be obtained as

$$P_{\text{loss,reactor}} = I_{\text{d}}^2 r_{\text{d}}. \tag{28}$$

7.4 DC-bias voltage source

The rectifier bridge and voltage transformer form a DC-bias voltage source, and the steady-state power loss resulting from this voltage source can be obtained as

$$P_{\text{loss,bias}} = P_{\text{core,SDT}} + i_{\text{SDT,rms}}^2 R_{\text{eq,SDT}} + I_{\text{d}} \cdot 2V_{\text{DF}}, \tag{29}$$

where $P_{\text{core,SDT}}$ is the step-down transformer core loss, $i_{\text{SDT,rms}}$ is the RMS value of the line current of the step-down transformer, and $R_{\text{eq,SDT}}$ is the equivalent resistance from the viewpoint of the primary side of the step-down transformer.

7.5 IGBT

IGBT is in on-state during the normal operation mode and conducts the DC reactor current. The steady-state power loss of IGBT can be shown as

$$P_{\text{loss, IGBT}} = V_{\text{SW}}I_{\text{d}}, \tag{30}$$

where V_{sw} represents the IGBT on-state voltage.

Combining Eqs. (26)–(30) results in the total steady-state power loss of the proposed SSFCL, which can be written as follows:

$$\begin{aligned} P_{\text{loss,SSFCL}} = {} & 4V_{\text{DF}}I_{\text{average}} + P_{\text{core,CT}} \\ & + R_{\text{eq,CT}}i_{\text{line,rms}}^2 + I_{\text{d}}^2 r_{\text{d}} + P_{\text{core,SDT}} \\ & + i_{\text{SDT,rms}}^2 R_{\text{eq,SDT}} + I_{\text{d}} \cdot 2V_{\text{DF}} + V_{\text{SW}}I_{\text{d}}. \end{aligned} \tag{31}$$

Considering Eq. (31), the SSFCL power losses can be reduced by reducing the resistance of the coil windings. However, in this study, it is assumed that the series transformer is ideal and that the transient inrush current on it is negligible. In addition, the DC-bias voltage source power loss is negligible. By this assumption, the total power losses of the proposed SSFCL are related to the DC reactor losses. As

discussed in Hagh and Abapour (2009b), the DC reactor optimized inductance value for the FCL application is about 0.2 H. By this inductance, it is possible to reduce the DC current ripple ($i_{r,p-p}$) to very low values, while the DC reactor resistance has a maximum value of 0.1 Ω (Hagh and Abapour, 2009b). Furthermore, the power loss in the DC reactor resistance is a very small percentage of the feeder power, and it is negligible for most of the practical applications.

8 Simulation results

In this section, the electrical network of Fig. 1 is simulated. The network parameters are listed in Table 1. The proposed network including SSFCL is simulated for normal and faulty operation modes. The fault condition is modeled by direct connection of single phase to ground. Also, the network source is solidly grounded.

Table 1 Network parameters

Parameter	Description	Value
V_s (simulation)	Source voltage (line-line), RMS	20 kV
r_s	Source resistance	1 Ω
L_s	Source inductance	0.01 H
f	Network frequency	50 Hz
V_{DF}	Voltage drop across power diode	2 V
V_{SW}	Voltage drop across IGBT	2 V
r_d	DC reactor resistance	0.1 Ω
R_p	Discharging resistor	50 Ω
L_d	DC reactor inductance	0.2 H
n_t	Isolation transformer turns ratio	1
R_{load}	Load resistance	48.4 Ω
L_{load}	Load inductance	0.1 H
r_f	Fault resistance	0 Ω
L_f	Fault inductance	0 H
C_{series}	Series capacitor	10 nF

8.1 SSFCL performance without using series RC branch and IGBT

Fig. 5 shows the line current during normal and faulty operation modes when there is no SSFCL connected to the line. During the normal mode, the line current is sinusoidal and its amplitude reaches 330 A. After fault inception, the first peak of the fault current increases rapidly and reaches 6880 A.

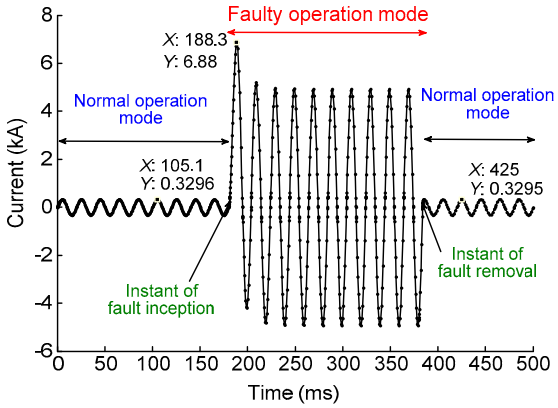

Fig. 5 Line current during the pre-fault, fault, and post-fault modes without using SSFCL

Fig. 6a shows the DC reactor current with a solid curve and line current with a dotted curve during the normal operation mode. In this case, IGBT is on and the series RC branch is bypassed thoroughly. Fig. 6b shows the expanded view of a portion of the line and DC reactor current for charging (t_0–t_2) and discharging (t_2–t_3) modes.

In this case, the SSFCL structure includes the DC reactor only and it is short-circuited via the DC voltage of the rectifier bridge. In this figure, the DC reactor current has a DC value with small AC ripple. This ripple can be reduced using a DC-bias voltage source (Fig. 6b).

At the fault inception, the DC reactor has limited the line current, and the line and DC reactor currents increase almost linearly. Small values of the DC reactor inductance cannot limit the fault current to an acceptable level. Comparison of Fig. 7 and Fig. 5 shows that the fault current amplitude decreases from 6880 A to 3948 A, which, however, is still a high value and may be dangerous for network equipment. By increasing the DC reactor inductance up to 0.5 H, the fault current decreases to the 2707 A level as shown with a dotted curve, but this value of the DC reactor increases the system loss, which is not acceptable. So, to have a compromise between system loss and SSFCL proper operation, we need to connect the series RC branch to the SSFCL structure via IGBT, which will be discussed in the following section.

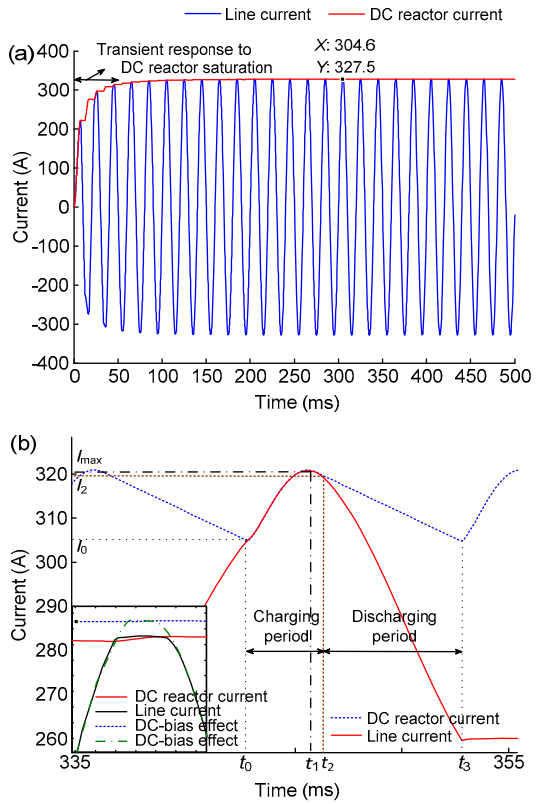

Fig. 6 DC reactor current in the normal operation mode while IGBT is on: (a) normal view; (b) expanded view

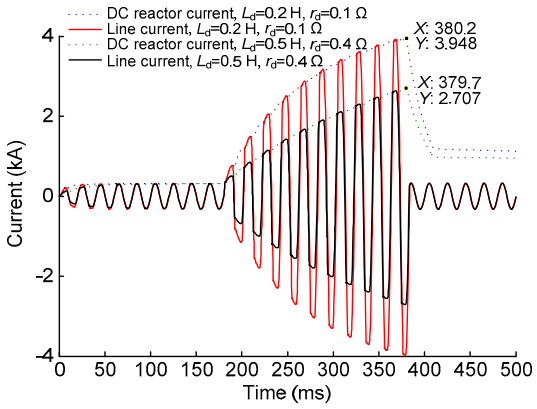

Fig. 7 Line and DC reactor currents in the normal, fault, and post-fault operation modes (IGBT and RC branch are not connected)

8.2 SSFCL performance using series RC branch and IGBT

To reduce the fault current below the threshold level (i_T), using a reduced reactor inductance value, the RC branch with controllable IGBT is added to the proposed SSFCL. By inserting the damping resistor of 50 Ω into the circuit, the acceptable current level is achieved, while the inductance of the reactor decreases to 0.2 H. So, there is a negligible delay and the problem of IGBT overvoltage is solved by using the RC branch as a snubber circuit. Fig. 8 shows the line current during normal and faulty operation modes when SSFCL is connected to the line.

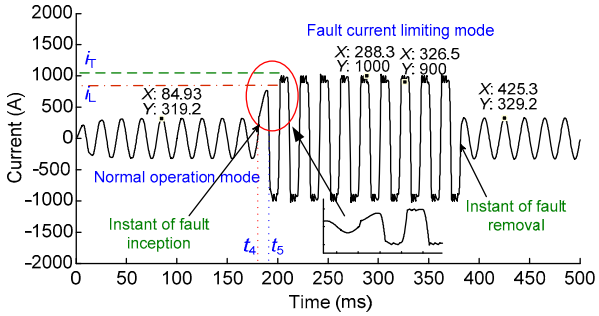

Fig. 8 Line current during the normal, fault, and post-fault operation modes with a proper duty cycle of IGBT

These results are obtained when the IGBT has an on-off duty cycle and the series RC branch is in series with the DC reactor. Before fault inception, the IGBT is on and the DC reactor freewheels via a rectifier bridge. After fault inception at t_4, as the fault current increases to above i_L, the control circuit turns off the IGBT and places the RC branch in series with the DC reactor at t_5, and accordingly the fault current decreases below i_T. By continuously turning on and off the IGBT, the fault current remains within a range around the specified level and the system is successfully protected against the fault. Fig. 9 shows the DC reactor and series RC branch current during normal and faulty operation modes. During normal operation, the series RC branch is bypassed and the DC reactor current is a direct current with a small ripple. Fig. 9a shows the effect of a series RC branch on the reactor current during the fault period. In this period, the IGBT connects the RC branch to the secondary side of the transformer and reduces the fault current to an acceptable level. Fig. 9b shows the DC reactor current when there is no connected RC branch. The impedance of the reactor can decrease the fault current to 4000 A, while in the case of using a series RC branch, the current amplitude decreases to 1000 A.

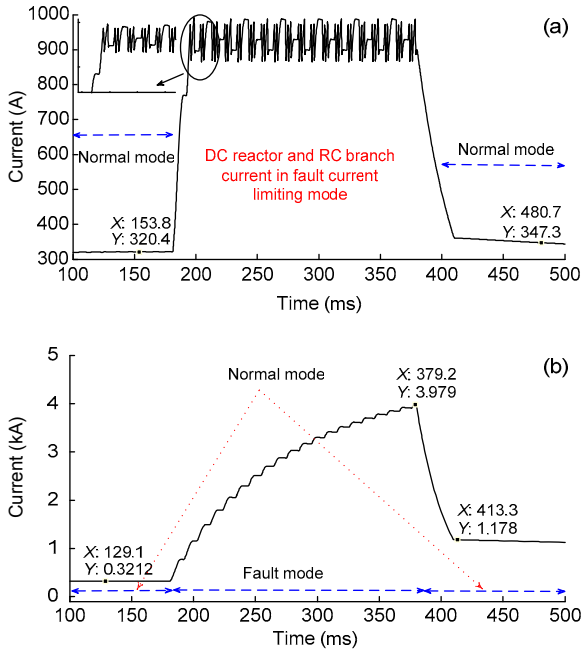

Fig. 9 DC reactor current during the normal, fault, and post-fault operation modes: (a) with RC branch effect and a proper duty cycle of IGBT; (b) without series RC branch effect

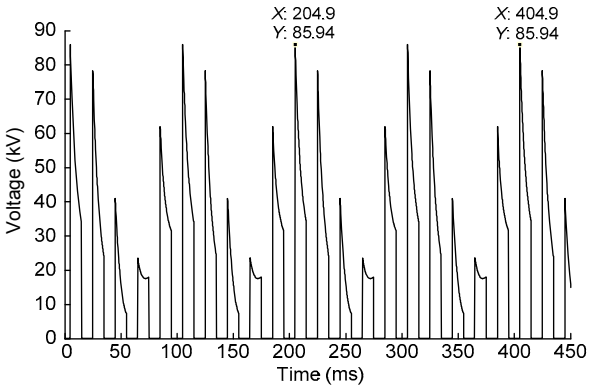

Fig. 10 IGBT overvoltage without using a series capacitor (only a damping resistor is connected in series with a reactor)

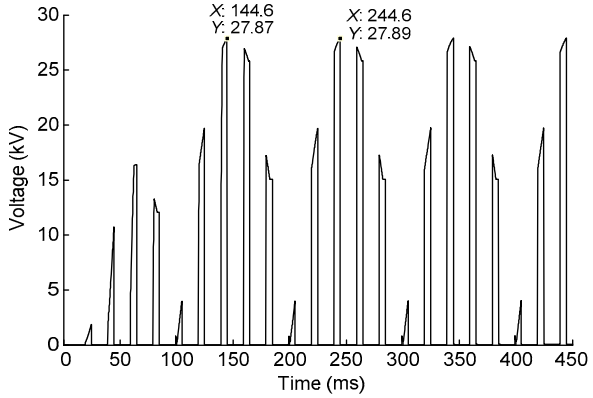

Fig. 11 IGBT overvoltage using a series capacitor, together with a damping resistor in series with a reactor

Fig. 10 shows the IGBT overvoltage when only a damping resistor is in parallel with the IGBT and there is no series capacitor in the SSFCL structure. In this case, the IGBT overvoltage rises above 80 kV, causing considerable voltage stress and power losses on the IGBT. In addition, the fault current amplitude is relatively high and causes high power losses on the damping resistor (Hagh and Abapour, 2009b).

Considering the switching overvoltage of FCL in Hagh and Abapour (2009b), considerable power loss on the IGBT occurs and in most cases, it can cause IGBT failure. By adding the series capacitor and resistor as a snubber circuit to the SSFCL structure, the switching overvoltage decreases (Fig. 11) and the resulting power loss on the IGBT decreases considerably. So, the snubber circuit can improve the SSFCL performance during the fault period. It is observed that the suggested SSFCL limits the switching overvoltage near the nominal peak voltage of the network. As the IGBT is turned on in the normal operation mode, the voltage drop across this switch is almost zero. However, during fault, the IGBT has on-off durations (Fig. 11).

Also, Fig. 12a shows the RMS value of the PCC voltage during normal and faulty operation modes. The dashed curve relates to the condition when no SSFCL is connected to the line. The dotted curve shows the PCC voltage when the IGBT and RC branches are not employed in the SSFCL structure. Therefore, only the DC reactor limits the fault current. The solid curve corresponds to the case with the proposed SSFCL, that is, using the RC branch and IGBT connected to the line. By comparing these curves, it is obvious that the SSFCL is able to retrieve the PCC voltage to an acceptable level. In addition, Fig. 12b shows the effects of the SSFCL operation on the sinusoidal PCC voltage during normal, fault, and post-fault modes. This waveform confirms that the SSFCL can fix the PCC voltage to an acceptable level during the fault period.

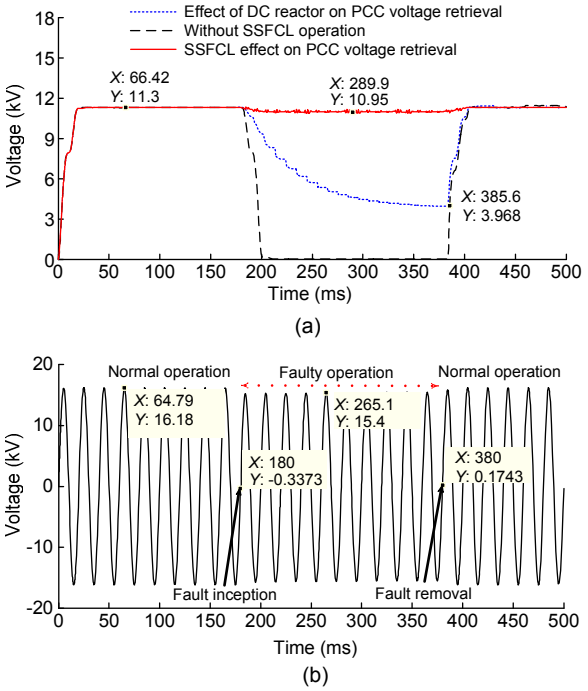

Fig. 12 PCC voltage during the normal and faulty operation modes: (a) RMS value with and without using SSFCL; (b) effect of SSFCL operation on the sinusoidal waveform of PCC voltage

9 Experimental results

Experimental results are obtained from a prototype circuit of the electrical network (Fig. 13). The prototype circuit parameters are listed in Table 2. This prototype consists of a DC reactor, control circuit, single-phase bridge rectifier, IGBT switch, and series RC branch. Using a start/stop switch, a single-line-to-ground fault is modeled. The controlling circuit includes a current sensor (LTS25-NP, LEM Company, USA), which is connected in series with the line for monitoring the line current during normal and faulty operation modes. The output of this sensor is applied to the microcontroller for evaluating the line current and producing the command signal for the IGBT. Fig. 14 shows the line current before and after fault occurrence when the SSFCL is connected in series with the line. The fault occurs at instant *a* and is removed at instant *b*. Before fault occurrence, the line current amplitude is 1.5 A (p-p) and the load voltage is 220 V (RMS).

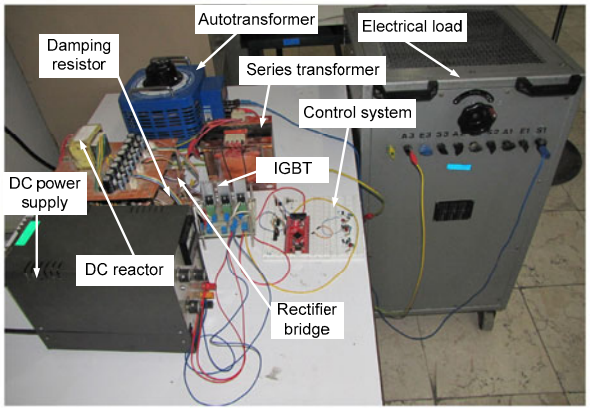

Fig. 13 SSFCL prototype structure

Table 2 Experimental setup parameters

Parameter	Value
Source voltage (line-line), V_s (RMS)	220 V
IGBT Infineon IKW40T120	
Voltage	1200 V
Current	40 A
Diode SKN 26/12	
Voltage	1200 V
Current	24 A
Distribution feeders	
Feeder F1	j0.314 Ω
Feeder F2	j0.157 Ω
Load	
Sensitive load	(10+j15.7) Ω
Load of F2	(410+j31.4) Ω
Reactor	
Inductance	0.2 H
Resistance	0.01 Ω
Capacitor	10 nF
Damping resistor	50 Ω
Fault inductance, L_f	0 H
Series capacitor, C_{series}	10 nF

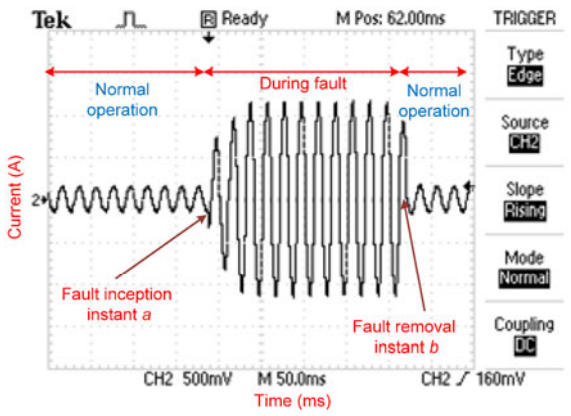

Fig. 14 SSFCL effect on line current during the normal, fault, and post-fault modes (current/division=500 mA with probe X3 and time/division=50 ms)

The line current is sinusoidal and the system works under a normal operation mode. In this case, the rectifier bridge short-circuits the DC reactor and the voltage drop on the SSFCL is negligible. In the faulty operation mode, by IGBT switching, the series RC branch is inserted into the line and the fault current decreases to 6.75 A (p-p) (Fig. 14). Fig. 14 is in fair agreement with Fig. 8. After fault removal, the current decreases to the normal value and again IGBT bypasses the RC branch.

Fig. 15 shows the line, series RC branch, and DC reactor currents during normal and faulty operation modes. Before fault inception, the reactor current is DC with a small ripple. After fault occurrence, the SSFCL topology changes by inserting the series RC branch into the line, which limits the fault current. After fault removal, the control circuit observes the current fall and turns the IGBT on. Also, Fig. 15a is in fair agreement with Fig. 6, and Figs. 15b and 15c are in fair agreement with Figs. 9a and 9b, respectively.

Fig. 16 shows the corresponding measured PCC voltage of the prototype system during normal and faulty operation modes. The measured PCC voltage is in agreement with that shown in Fig. 12b. The measured PCC voltage before fault is 220 V (RMS) and SSFCL has no effect on the network power quality. During the faulty operation mode, SSFCL has prevented severe voltage drop and has restored PCC voltage at an acceptable level.

The advantages of the proposed SSFCL are as follows: Compared with Hagh and Abapour (2009b) and Firouzi *et al*. (2013), the proposed SSFCL uses a series RC branch as a snubber to decrease the IGBT switching overvoltage, which leads to better switching of the IGBT and less power loss in the fault period. Though the DC-bias voltage source is inserted in series with the DC reactor, the SSFCL will not cause any power quality loss during the steady state. Also, by adding the snubber circuit to the SSFCL structure, the configuration of SSFCL remains simple and reliable. Decreasing the IGBT overvoltage during the fault makes the proposed SSFCL reliable and practical; accordingly, the duration of the SSFCL operation during the fault period can be increased. So, it can also reduce the interruption rating of the circuit breaker.

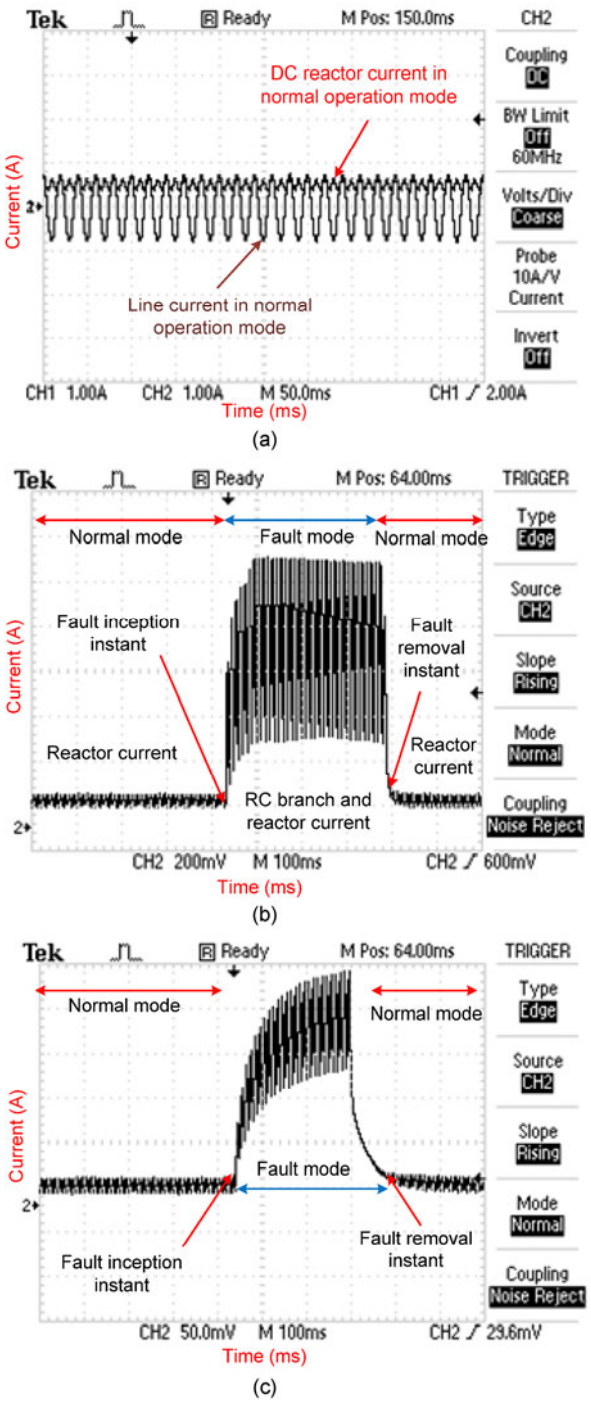

Fig. 15 Line, series RC branch, and DC reactor currents during normal and faulty operation modes

(a) Line and reactor currents in the normal operation mode (current/division=1 A with probe X1 and time/division=50 ms); (b) Series RC branch and IGBT current in normal and faulty operation modes (current/division=200 mA with probe X6 and time/division=100 ms); (c) DC reactor current in normal and faulty operation modes (current/division=50 mA with probe X100 and time/division=100 ms)

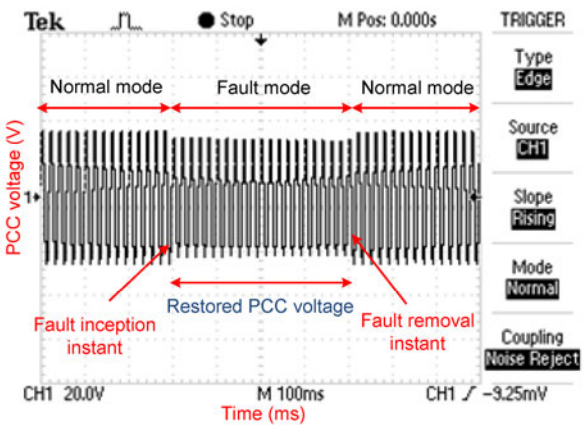

Fig. 16 PCC voltage during the normal, fault, and post-fault modes (voltage/division=20 V with probe X20 and time/division=100 ms)

10 Conclusions

In this paper, an improved SSFCL configuration has been proposed. The main advantages of the proposed SSFCL are its lower switching overvoltage compared with similar structures, lower initial cost, acceptable power losses, and reduction of the inductance and current rating of the DC reactor. Due to the control of the DC reactor current, there is no need for a disconnecting switch. Also, using the lower DC reactor, the power losses are compensated and the SSFCL has no effect on the utility voltage or load current. Adding the snubber circuit to the SSFCL structure reduces the IGBT overvoltage during the fault period, and the power losses decrease as well. This leads to a reduced cooling system and as a result, the system's initial cost decreases. Note that the SSFCL structure is simple and results in better power quality. Simulation and experimental results indicate the good performance of the proposed SSFCL.

References

Abramovitz, A., Smedley, K.M., 2012. Survey of solid-state fault current limiters. *IEEE Trans. Power Electron.*, **27**(6):2770-2782. [doi:10.1109/TPEL.2011.2174804]

Amanulla, B., Chakrabarti, S., Singh, S.N., 2012. Reconfiguration of power distribution systems considering reliability and power loss. *IEEE Trans. Power Deliv.*, **27**(2): 918-926. [doi:10.1109/TPWRD.2011.2179950]

Cheng, S., Chen, M.Y., Wai, R.J., *et al.*, 2014. Optimal placement of distributed generation units in distribution systems via an enhanced multi-objective particle swarm optimization algorithm. *J. Zhejiang Univ.-Sci. C (Comput. & Electron.)*, **15**(4):300-311. [doi:10.1631/jzus.C1300250]

Cvoric, D., de Haan, S.W.H., Ferreira, J.A., 2008. Comparison of the four configurations of the inductive fault current limiter. IEEE Power Electronics Specialists Conf., p.3967-3973. [doi:10.1109/PESC.2008.4592574]

Du, H.I., Kim, Y.J., Lee, D.H., *et al.*, 2011. Effect of the resistance of two different coated conductors on the current-limiting performance of flux-lock type superconducting fault current limiters. *IEEE Trans. Appl. Supercond.*, **21**(3):1254-1257. [doi:10.1109/TASC.2011.2104350]

Fani, B., Hamedani Golshan, M.E., Askarian Abyaneh, H., 2011. Waveform feature monitoring scheme for transformer differential protection. *J. Zhejiang Univ.-Sci. C (Comput. & Electron.)*, **12**(2):116-123. [doi:10.1631/jzus.C1010042]

Firouzi, M., Gharehpetian, G.B., Pishvaei, M., 2013. A dual-functional bridge type FCL to restore PCC voltage. *Int. J. Electr. Power Energy Syst.*, **46**:49-55. [doi:10.1016/j.ijepes.2012.09.011]

Ghanbari, T., Farjah, E., 2013. Unidirectional fault current limiter: an efficient interface between the microgrid and main network. *IEEE Trans. Power Syst.*, **28**(2):1591-1598. [doi:10.1109/TPWRS.2012.2212728]

Globalspec, 2015. The Engineering Search Engine. Globalspec, Inc., USA. Available from http://www.globalspec.com

Hagh, M.T., Abapour, M., 2007. DC reactor type transformer inrush current limiter. *IET Electr. Power Appl.*, **1**(5):808-814. [doi:10.1049/iet-epa:20060511]

Hagh, M.T., Abapour, M., 2009a. Non-superconducting fault current limiters. *Eur. Trans. Electr. Power*, **19**(5):669-682. [doi:10.1002/etep.247]

Hagh, M.T., Abapour, M., 2009b. Nonsuperconducting fault current limiter with controlling the magnitudes of fault currents. *IEEE Trans. Power Electron.*, **24**(3):613-619. [doi:10.1109/TPEL.2008.2004496]

Hanif, A., Choudhry, M.A., 2009. Dynamic voltage regulation and power export in a distribution system using distributed generation. *J. Zhejiang Univ.-Sci. A*, **10**(10): 1523-1531. [doi:10.1631/jzus.A0820699]

Iwahara, M., Mukhopadhyay, S.C., Yamada, S., *et al.*, 1999. Development of passive fault current limiter in parallel biasing mode. *IEEE Trans. Magn.*, **35**(5): 3523-3525. [doi:10.1109/20.800577]

Jafari, M., Naderi, S.B., Hagh, M.T., *et al.*, 2011. Voltage sag compensation of point of common coupling (PCC) using fault current limiter. *IEEE Trans. Power Deliv.*, **26**(4): 2638-2646. [doi:10.1109/TPWRD.2011.2161496]

Jang, J.Y., Park, D.K., Yang, S.E., *et al.*, 2010. A study on the non-inductive coils for hybrid fault current limiter using experiment and numerical analysis. *IEEE Trans. Appl. Supercond.*, **20**(3):1151-1154. [doi:10.1109/TASC.2010.2041219]

Liu, J.M., Fan, T.R., Tong, K.Z., 2007. Research of network technology for intelligent circuit breaker controller. *J. Zhejiang Univ.-Sci. A*, **8**(3):464-468. [doi:10.1631/jzus.2007.A0464]

Madani, S.M., Rostami, M., Gharehpetian, G.B., *et al.*, 2013. Improved bridge type inrush current limiter for primary grounded transformers. *Electr. Power Syst. Res.*, **95**:1-8. [doi:10.1016/j.epsr.2012.08.012]

McAullife, J., Amin, D., Peacock, I., *et al.*, 2001. Optimizing capital costs in power-distribution upgrades. *IEEE Ind. Appl. Mag.*, **7**(5):41-51. [doi:10.1109/2943.948531]

Na, J.B., Kim, Y.J., Jang, J.Y., *et al.*, 2012. Design and tests of prototype hybrid superconducting fault current limiter with fast switch. *IEEE Trans. Appl. Supercond.*, **22**(3):5602604. [doi:10.1109/TASC.2011.2182334]

Radmanesh, H., Fathi, S.H., Gharehpetian, G.B., 2015a. Novel high performance DC reactor type fault current limiter. *Electr. Power Syst. Res.*, **122**:198-207. [doi:10.1016/j.epsr.2015.01.005]

Radmanesh, H., Fathi, S.H., Gharehpetian, G.B., 2015b. Series transformer based solid state fault current limiter. *IEEE Trans. Smart Grid*, **6**(4):1983-1991. [doi:10.1109/TSG.2015.2398365]

Tsuda, M., Mitani, Y., Tsuji, K., *et al.*, 2001. Application of resistor based superconducting fault current limiter to enhancement of power system transient stability. *IEEE Trans. Appl. Supercond.*, **11**(1):2122-2125. [doi:10.1109/77.920276]

Vintan, M., 2008. Evaluating transmission towers potentials during ground faults. *J. Zhejiang Univ.-Sci. A*, **9**(2):182-189. [doi:10.1631/jzus.A072206]

Wu, Z.L., Chen, P.P., Tan, L.Y., *et al.*, 2001. Short circuit current limiter in AC network. *J. Zhejiang Univ.-Sci.*, **2**(1):41-45. [doi:10.1631/jzus.2001.0041]

Yamaguchi, H., Kataoka, T., 2008. Current limiting characteristics of transformer type superconducting fault current limiter with shunt impedance and inductive load. *IEEE Trans. Appl. Supercond.*, **18**(2):668-671. [doi:10.1109/TASC.2008.921258]

Ye, L., Lin, L.Z., Juengst, K.P., 2002. Application studies of superconducting fault current limiters in electric power systems. *IEEE Trans. Appl. Supercond.*, **12**(1):900-903. [doi:10.1109/TASC.2002.1018545]

Zhao, C., Lu, J.Z., Fang, Z., *et al.*, 2010. Study of a novel fault current limiter on the basis of high speed switch and triggered vacuum switch. 5th Int. Conf. on Critical Infrastructure, p.1-5. [doi:10.1109/CRIS.2010.5617487]